Biochimica et Biophysica Acta, 440 (1976) 107–121

BBA 47129

ENERGY TRANSFER IN PHOTOSYNTHESIS

KONRAD COLBOW and R. P. DANYLUK

Department of Physics, Simon Fraser University, Burnaby, B.C. V5A 1S6 (Canada)

(Received November 28th, 1975)

SUMMARY

A theoretical model is presented to account for the physical mechanism of energy transfer from antenna molecules to the reaction centers in photosynthesis. The energy transfer is described by a generalized transport equation or "master equation". The solution of this equation for the proposed model gives a relationship between the antennae interaction energy and the transfer rate. The results are shown to be in agreement with inter-antenna transfer rates calculated from experimental fluorescence lifetimes. Previous theories were based either on the Förster mechanism, which is valid for very small interaction energies, or an exciton model valid for very large interactions, but experimental results seemed to indicate that the actual situation was intermediate between these two. The Förster theory and the exciton model are limiting cases of the master equation.

I. INTRODUCTION

Chlorophyll *a* and its auxiliary pigments (mainly carotenoids) absorb light energy and transfer at low light excitation intensity about 97 % of it to reaction centers, where water is split (System II) and the reducing agent NADPH is produced (System I). This is known as the light reaction and it takes place in the closed vesicle forming thylakoid membranes inside the chloroplasts of higher plants. In a following dark reaction outside the membranes CO_2 is then reduced to carbohydrate with the aid of NADPH and free energy stored in the molecules of ATP. About 3 % of the absorbed light is re-emitted as fluorescence within nanoseconds. The decay time and yield of this fluorescence depends either on the efficiency of energy uptake by the reaction center, or on the time required for light energy to reach the reaction center, or possibly on both [1].

Traditionally, the theory of energy transfer between molecules has been discussed in the limits of strong (Perrin's theory) and very weak intermolecular coupling energy (Förster's theory) [2, 3]. The terms strong and very weak apply relative to the vibrational energy levels within the individual molecules. The intermediate or weak coupling region was too difficult to treat mathematically [3]. The energy transfer rate is proportional to the interaction energy in Perrin's theory and to the square of the interaction energy in Förster's theory. In the model of a dipole-dipole interaction

energy this leads to a R^{-3} and R^{-6} dependence of the transfer rate on the molecular spacing for the two theories, respectively. Rather than expressing the range of applicability in terms of the interaction energy we may also state that the Förster or the Perrin theory is applicable if the transfer rate is slow or fast compared to the thermal relaxation rate in the vibrational levels of an individual molecule.

In a recent paper Colbow [1] has shown that approximate agreement of the calculated and the observed fluorescence decay was obtained by using the Förster theory, the assumption of an "open-trap" reaction center at low light excitation intensity, and a 2-dimensional random walk among 300 antenna chlorophyll per reaction center. If one divides the low excitation fluorescence lifetime of 0.4 ns by the average number of steps required for the excitation to reach the reaction center, one obtains a nearest neighbor transfer rate of $1.5 \times 10^{12}\ s^{-1}$. Using a mean chlorophyll spacing of 15 Å and a Förster parameter of $R_0 = 65$ Å, Colbow [1] calculated a nearest neighbor transfer rate of $0.44 \times 10^{12}\ s^{-1}$. These rates seemed reasonably close to give some confidence in the general correctness of the model. Both rates were below the thermal relaxation rate of $3 \times 10^{12}\ s^{-1}$ which justified using the Förster theory rather than Perrin's theory [1]. However, the rate is sufficiently close to the thermal relaxation rate to warrant a closer look at the applicability of the Förster theory in photosynthesis [4, 5].

Kenkre and Knox [6] have developed an approach based on the "generalized master equation" that allows one to calculate the transfer rate in terms of interaction energy over a wide range of coupling strengths. A relationship is obtained in terms of well-defined spectral properties of the isolated molecule, such as lineshape and half-width of the absorption band, and the Stoke's shift of the fluorescence. The strong and very-weak coupling cases are readily obtained in the appropriate limits of the master-equation solution, while a continuous relationship between transfer rate and interaction energy is provided throughout the intermediate weak region.

II. A MODEL OF THE PHOTOSYNTHETIC UNIT

The model of the photosynthetic unit that we will be using consists of an array of chlorophyll molecules embedded in a fluid lipid bilayer membrane. We will assume that the lipids and the globular proteins in the membrane have little influence on energy transfer between chlorophyll molecules other than by acting as a medium of uniform index of refraction, and providing a thermal bath [1, 8]. We will assume the antenna chlorophyll are of one type, chlorophyll *a*. Other pigments such as chlorophyll *b* and carotenoids absorb light at shorter wavelengths and pass the energy almost irreversibly to the chlorophyll *a* antennae. In this way they extend the absorption spectrum of the plant over most of the visible region. The antenna chlorophyll *a* can thus be excited either by direct absorption or by energy transfer from these other pigments. In bacteria, bacteriochlorophyll acts as antenna, analogous to chlorophyll *a*.

The lipid-protein membrane will be assigned an average index of refraction of $n = 1.45$ [1, 9], the refractive index of lipid-like materials.

The structure of chlorophyll *a* has been shown previously [1]. The absorption spectrum of a dilute solution of chlorophyll *a* in ether [10] shows two main absorption bands, the Soret band around 430 nm and the red band around 660 nm. These bands are the result of singlet electronic transitions of the delocalized π electrons around the

porphyrin ring. Studies of dichroism have shown that the dipole moments of these transitions lie in the plane of the porphyrin ring of the chlorophyll *a* molecule [11]. The hydrocarbon phytol chain does not appreciably affect either the band shape or the position of the absorption bands [12].

The red band is the one responsible for energy transfer among chlorophyll *a* antennae to the reaction center. Energy absorbed in the Soret band is rapidly degraded by intermolecular vibrations and transferred to the red band. No fluorescence can be observed corresponding to the Soret band.

The main transition of the red band is at 660 nm with a vibrational satellite at 613 nm. The transition moments for these are oriented along the long axis from ring I to III of the porphyrin head (see Fig. 2 in Ref. 1). They are referred to in the literature as Q_y $(0 \leftarrow 0)$ and Q_y $(1 \leftarrow 0)$. Weak peaks at 575 nm and 530 nm are also singlet $\pi\pi^*$ transitions with transition moments perpendicular to the Q_y bands along the shorter porphyrin axis (ring II to IV). However, their contribution is not significant for our considerations. In Fig. 1 the 660 nm and 613 nm bands are fitted with Gaussian and Lorentzian profiles. It is readily seen that the 660 nm band is nearly Gaussian in shape. The 613 nm band is difficult to fit because of its small size, but is most likely Gaussian as well. The fluorescence spectrum is nearly a mirror image of the 660 and 613 nm bands [12]. The emission maximum is located at 668 nm giving a Stoke's shift of 161 cm^{-1} [1].

The spectrum of chlorophyll *a* in vivo is more complex than that of chlorophyll *a* in dilute solution. Instead of one main red band at about 660 nm in solution, a band with components at 673, 683, and 695 nm is observed in vivo [11, 13]. The dichroism of the in vivo spectrum is very weak except for the 695 component*. This implies either a random orientation [12] of the porphyrin rings in the membrane, or chlorophyll *a*

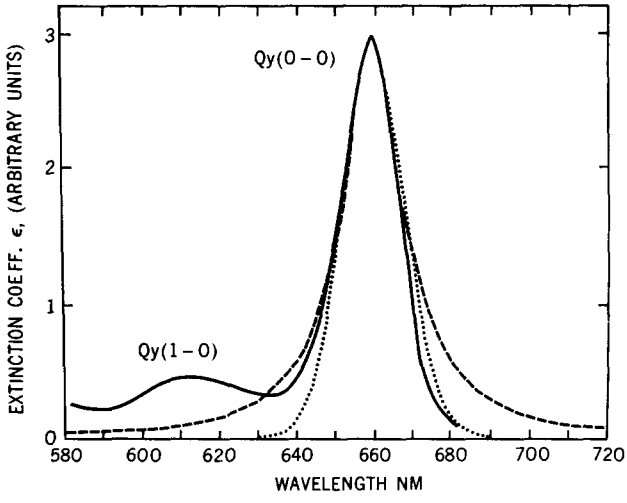

Fig. 1. Gaussian (dotted line) and Lorentzian (dashed line) profiles fitted to the red absorption band of chlorophyll *a* in ether. Data (solid line) from French [10].

* In artificially oriented chloroplasts stronger dichroism has recently been observed for the other red bands [33].

is anchored by the phytol chain in the membrane with the red and blue transition moment at an angle of 35.3° with the membrane plane, but free to rotate azimuthally [13]. Then with the red and blue transitions at right angles to each other, the plane of the porphyrin head is inclined at an angle of 54.7° to the membrane plane [13]. Direct measurements of chlorophyll *a* orientation in artificial membranes have also been made. Using lipid bilayers, Steinemann et al. [14] measured the red transition moment as being oriented at $35\pm2°$ and the blue transition moment at $26\pm3°$ to the membrane plane (averaged values for three lipids). They determined the inclination of the porphyrin plane as being $46\pm5°$ to the membrane surface. Cherry et al. [15] determined corresponding angles of 36.5°, 26° and 48°. Hoff [16] using lecithin multilayers measured the orientation of the red transition moment as $34.3\pm1.1°$ and the inclination of the porphyrin plane as $55.4\pm1°$ with the membrane plane. We shall use an average value of $35\pm2°$ for the angle of the red transition moment with the membrane plane. The inclination of the porphyrin plane does not enter into our calculations. It seems reasonable to assume that the porphyrin head is in the hydrocarbon region of the membrane rather than in the polar region [14]. This information cannot be deduced from dichroism measurements. The argument is based on the fact that the larger part of the porphyrin ring is hydrophobic except for the $-COOCH_3$ and C=O groups of the cyclopentanone ring which should make contact with the water-lipid interface.

To determine the mean spacing of chlorophyll *a* antenna Wolken and Schwertz [17], using electron microscopy, measured an available area of 222 and 246 $Å^2$ per chlorophyll molecule in the chloroplasts of *Euglena gracilis* and *Poteriochronmonas stipitata*. Thomas et al. [18] measured a range of 90 to 360 $Å^2$ for grana-bearing chloroplasts; their average is 240 $Å^2$. Kreutz [13] using X-ray diffraction measured an average area of 215 $Å^2$ per chlorophyll. For our model we choose a range of 200 to 250 $Å^2$ corresponding to a mean-spacing of 15 ± 1 Å between chlorophyll molecules [1].

Next we need to know in our model the number of antenna chlorophyll associated with a trap. Emerson and Arnold [19] showed that about 2400 chlorophyll molecules were involved in the evolution of one oxygen molecule. There is evidence that 8 photons are needed in this process [20], which gives a value of 300 chlorophyll *a* per reaction center, assuming an even division between Photosystem I and II. One sometimes finds lower values such as 100 being used without justification [4]*. Schmid and Gaffron [21] have recently repeated the Emerson and Arnold experiment measuring the amount of $^{14}CO_2$ fixed per saturating flash. They vindicated the value of 2400 for normal, healthy plants, but showed that the size of the photosynthetic unit could vary in discrete steps of 300 chlorophyll around the value of 2400. This may be due to inactive reaction centers. In chlorophyll deficient mutants, units as small as 1/8 of this value were found. In chlorophyll-rich adult plants and algae most of the unit sizes were between 2000 and 2700. Thus considering the variability of unit size and the uncertainty in partitioning of the antenna chlorophylls between the two photosystems, we have chosen a range of 250 to 350 antenna chlorophyll *a* per reaction center in our model calculations.

It will be assumed that excitation in the photosynthetic unit can either be

---

* Depending on growth conditions such a low number is found in photosynthetic bacteria. However, the lack of other experimental parameters (i.e. chlorophyll spacing) makes it impossible to analyze bacteria fluorescence in terms of our present model.

trapped by a reaction center or lost as fluorescence. Interconversion processes such as singlet to triplet transitions leading to non-radiative de-excitation in the antenna chlorophyll are considered to be negligible. We shall also assume that energy once trapped does not return to the antenna chlorophyll since the trap absorbs light at a longer wavelength (680 nm for Photosystem II) [8] than the antenna chlorophyll *a*. Hoch and Knox [22] estimate a value of 10^{-4} for the ratio of out to in jump probabilities. The trap itself is believed to be a specialized form of chlorophyll *a* aggregated with a protein.

With all traps "open" the fluorescence from the antenna is at a minimum as the traps compete with fluorescence for the excitation and thus quench the fluorescence. The fluorescence decay-time is then the same as the time needed for the excitation to reach the trap. This condition is obtained experimentally by using low light levels, thus avoiding saturation. Müller et al. [23] have shown that the fluorescence lifetime reaches limiting values for both high and low light intensities. The saturation value is 1.92 ns while the lifetime approaches a value of about 0.35 ns for low light intensity*. These findings are consistent with the assumed mechanism in which energy absorbed by chlorophyll *a* is transferred to the trapping centers by a singlet state resonance mechanism. After receiving a quantum of energy the traps are unable to accept energy until they have completed the photochemical process. At very low light intensity the traps are unoccupied on average, thus the excitation quanta are trapped rapidly, resulting in a short fluorescence lifetime. At high light intensity, or under conditions of chemically poisoned traps, the traps are occupied or not functional, so that excitation resides in the antenna chlorophyll for longer periods of time, resulting in an increased fluorescence lifetime.

The 5-fold increase of fluorescence with light intensity is strong evidence that a considerable part of the energy is delivered to the traps via singlet excited states. If the energy transfer was by triplet states, little fluorescence increase would be expected, as fluorescence is the result of radiative decay of singlet energy levels [4, 24]. Measurements of fluorescence lifetime prior to Müller et al. were done at unspecified excitation intensities and the results range in value from 0.6 to 1.7 ns [23]. The limiting values were probably not observed because not sufficient consideration was given to the level of the exciting intensity [23].

The saturating value appears to be universal in plants [23]. The open-trap value is also the same for blue and red algae [25]. Thus we shall adopt the value of 0.4 ± 0.1 ns as the open-trap fluorescence lifetime and interpret it as the trapping time of excitation.

What we have described applies only to Photosystem II. The fluorescence from Photosystem I decays about ten times faster than that from Photosystem II and only recently have accurate measurements been made [4, 5]. There also seems to be an absence of fluorescence that varies with the state of the traps in Photosystem I, and it has been suggested that energy transfer takes place via triplet states [4, 26]. In short, the behaviour of Photosystem I is not as well understood as that of Photosystem II.

---

* Lifetimes shorter than this have been reported recently [34, 35].

III. THE MASTER EQUATION APPROACH

The Pauli master equation

$$dP_i(t)/dt = \sum_j [F_{ij}P_j(t) - F_{ji}P_i(t)] \tag{1}$$

describes the probability of excitation at molecule P_i as a function of probabilities of excitation at the other molecules (P_j) and transition probability rates F_{ij}. The equation is Markoffian, which means that the probability F_{ij} of excitation jumping from i to j is independent of its previous location. This is applicable to very-weak coupling where the excitation can be considered as localized on a particular site before hopping to the next site. The jump times would then be given by the Förster formulation and the trapping time could be worked out by solving the set of coupled Pauli master equations for the array of molecules [27]. This is equivalent to a random walk, for which Montroll [28] has worked out analytic equations in one, two and three dimensions; the results are essentially the same as those obtained from the Pauli master equation.

The non-Markoffian generalized master equation [6]

$$\frac{dP_i(t)}{dt} = \int_0^t ds \sum_j \{w_{ij}(t-s)P_j(s) - w_{ji}(t-s)P_i(s)\} \tag{2}$$

contains the strong and very weak regions as limits and also holds in the intermediate region. Here the probability of transition depends on where the excitation was before t; w_{ij} connects the probability at a site j at time s in the past to the rate change of probability at site i at the present time t. By substituting

$$w_{ij}(t-s) = F_{ij}\delta(t-s) \tag{3}$$

into the generalized master equation one obtains the Pauli master equation. The delta function means that the transition probability depends on what happens at time t, not on previous history. The Pauli master equation thus eliminates the possibility of exciton or reversible resonance coupling between molecules.

A useful, more general, approximation is to assume that the time dependence of w_{ij} is independent of the sites i and j:

$$w_{ij}(t) = F_{ij}\phi(t) \tag{4}$$

where $\phi(t)$ is called the memory function. The generalized master equation then reduces to

$$dP_i(t)/dt = \int_0^t ds\phi(t-s)[\sum_j \{F_{ij}P_j(s) - F_{ji}P_i(s)\}] \tag{5}$$

$\phi(t)$ defines the extent in time in which the process can be considered non-Markoffian. Kenkre and Knox [6] derived the expression

$$\phi(t) = [1/\pi f(0)] \int_{-\infty}^{\infty} f(\Delta\nu)\cos(\Delta\nu t)d(\Delta\nu) \tag{6}$$

where $f(0)$ is the Förster rate equation for two molecules in terms of their overlap of fluorescence and absorption:

$$f(0) \propto 1/R^6 \int_0^\infty [\varepsilon(\nu)\varepsilon(2\nu_0-\nu)/\nu(2\nu_0-\nu)]\mathrm{d}\nu \tag{7}$$

$\varepsilon(\nu)$ is the extinction coefficient and ν_0 the average frequency of absorption and fluorescence maximum. $f(\Delta\nu)$ is given by the same equation as $f(0)$ but the peaks are shifted on the frequency scale by $+\Delta\nu/2$ for the emission and $-\Delta\nu/2$ for the absorption. Physically this represents a molecule that has not come to full thermal equilibrium before transferring energy. Thermal equilibrium would imply the full Stokes shift ν_s between the fluorescence and absorption peak.

If the peaks are nearly symmetrical the denominator is equal to $\nu_0{}^2$ and can be removed from the integral. We obtain

$$f(0) = K\int_0^\infty \varepsilon(\nu)\varepsilon(2\nu_0-\nu)\mathrm{d}\nu \equiv KJ_0$$

$$f(\Delta\nu) = K\int_0^\infty \varepsilon\left(\nu-\frac{\Delta\nu}{2}\right)\varepsilon\left(2\nu_0-\nu+\frac{\Delta\nu}{2}\right)\mathrm{d}\nu \equiv KJ(\Delta\nu) \tag{8}$$

where J_0 is the overlap of the absorption and fluorescence, $J(\Delta\nu)$ is the shifted overlap of the absorption and effective emission peak, and K contains the remaining terms.

The memory function then becomes

$$\phi(t) = (\pi J_0)-1\int_{-\infty}^\infty J(\Delta\nu)\cos(\Delta\nu t)\mathrm{d}\Delta\nu \tag{9}$$

Assuming mirror image symmetry between the absorption and fluorescence bands and using Eqns. 8 and 9 we obtain for a Gaussian and Lorentzian profile the normalized memory functions [i.e. $\phi(0) = 1$]

$$\phi(t) = \begin{cases} \exp(-\alpha_G^2 t^2)\cos(\nu_s t) & \text{Gaussian} \\ \exp(-\alpha_L t)\cos(\nu_s t) & \text{Lorentzian} \end{cases} \tag{10}$$

$$\alpha_G = 0.85\nu_{\frac{1}{2}} \quad \text{and} \quad \alpha_L = 2.0\nu_{\frac{1}{2}}$$

Here $\nu_s = 2(\nu_a-\nu_0)$ is the Stoke's shift, ν_a is the wave number of the absorption maximum, and $\nu_{\frac{1}{2}}$ is the halfwidth at half maximum. $\phi(t)$ is plotted in Fig. 2 for chlorophyll *a* in ether using a value of $\nu_{\frac{1}{2}} = 188\ \mathrm{cm}^{-1}$, $\nu_s = 161\ \mathrm{cm}^{-1}$ and the Gaussian and Lorentzian approximation for the main peak at 660 nm. α is a measure of how fast the localization of excitation takes place. For excitation lifetimes greater than $1/\alpha$ the energy transfer process can be considered Markoffian. For times much greater than $1/\alpha$, $\phi(t) \approx \delta(t)$ and the generalized master equation reduces to the Pauli master equation describing a random hopping of excitation. Thermal relaxation occurs in about 3×10^{-13} s, and $\phi(t)$ has become small by this time (Fig. 2). This indicates that thermal relaxation has destroyed all phase relationship between the excitation on neighboring molecules, thus effectively randomizing the transfer process. If $\phi(t)$ is not zero for times larger than the thermal relaxation time one must have a small α and therefore a narrow line width. This is possible for systems that have discrete sharp vibrational bands, and thus weaker interactions with phonons and the environment and a correspondingly longer memory [6]. Chlorophyll has a continuous spectrum. Therefore it couples very readily to the environment, which is reflected in its wider band width and shorter memory.

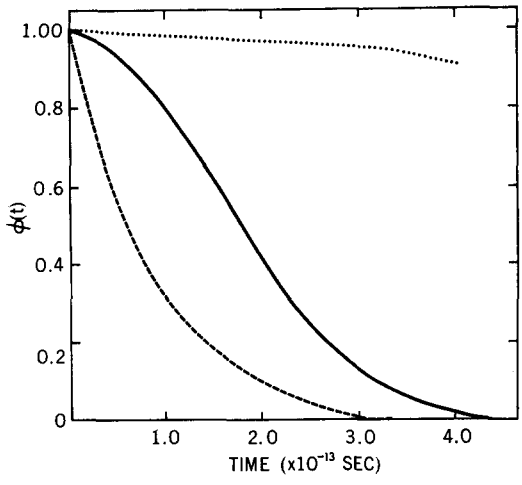

Fig. 2. The memory function $\phi(t)$ versus time for a Gaussian (solid line) and Lorentzian (dashed line) profile. The cosine variation (dotted line) is negligible in Eqn. 10 compared to the exponential factor.

IV. SOLUTION OF THE GENERALIZED MASTER EQUATION

Having obtained the memory function we can now calculate the mean square displacement of excitation and relate the transfer rate and interaction energy for Gaussian and Lorentzian profiles. If the molecules have an average spacing a, the mean square displacement of the excitation is

$$\langle x^2 \rangle = (\sum_m m^2 a^2 P_m) / \sum_m P_m = \langle m^2 \rangle a^2 \tag{11}$$

where P_m, the probability that the excitation is on molecular site m, obeys the generalized master equation. The rate of excitation transfer w is the inverse of the time required for $\langle x^2 \rangle$ to build up from zero to the value a^2. This leads to the equation [6, 7]

$$a^2 = \langle A \rangle \int_0^{1/w} dt \int_0^t \phi(s) ds, \tag{12}$$

where

$$\langle A \rangle = [\sum_n P_n \sum_m F_{mn}(m-n)^2 a^2] / \sum_n P_n$$

The time dependent transition rates of the generalized master equation have the form [7]

$$w_{mn}(t-s) \equiv F_{mn}\phi(t-s) = (2u^2/\hbar^2)\phi(t-s) \tag{13}$$

where u is the interaction energy between sites m and n. Thus using Eqn. 10 we write

$$F_{mn}\phi(t) = (2u^2/\hbar^2)e^{-Z} \tag{14}$$

where $Z = \alpha_G{}^2 t^2$ for a Gaussian and $Z = \alpha_L t$ for a Lorentzian profile. We have

dropped the cosine terms because of their negligible contribution. We now solve Eqn. 12 for nearest neighbor interactions on a square lattice. In this case $P_n = \frac{1}{4}$ and $\sum_n P_n = 1$. Summing over the four nearest neighbors, and substituting into Eqn. 14, we obtain for the Gaussian profile

$$2(u/\hbar)^2 \int_0^{1/w} dt \int_0^t e^{-\alpha_G{}^2 s^2} ds = 1 \tag{15}$$

which gives

$$\sqrt{\pi}\left(\frac{\alpha_G}{w}\right) \operatorname{erf}\left(\frac{\alpha_G}{w}\right) + e^{-\alpha_G{}^2 w^2} - 1 = \left(\frac{\alpha_G \hbar}{u}\right)^2 \tag{16}$$

This equation relates the nearest neighbor transfer rate w to the interaction energy u and the spectral half-width of the molecules involved. For very-weak coupling ($\alpha_G \gg |u|/\hbar$) the error function (erf) approaches one and the exponential zero. In this case Eqn. 16 gives $w = \sqrt{\pi}\, u^2/\alpha_G \hbar^2$. For strong coupling ($\alpha \ll |u|/\hbar$), $\operatorname{erf}(\alpha_G/w) \approx (2\alpha/\sqrt{\pi}w)$ and $\exp(\alpha_G/w)^2 \approx 1-(\alpha_G/w)^2$, this leads to $w = |u|/\hbar$. Thus Eqn. 21 gives the correct results in the fast and slow limits of energy transfer and provides a connecting formula for the intermediate region.

For a Lorentzian profile we obtain analogous to Eqn. 16, in agreement with Kenkre and Knox [6]

$$e^{-\alpha_L/w} + \frac{\alpha_L}{w} - 1 = \tfrac{1}{2}\left(\frac{\alpha_L \hbar}{u}\right)^2 \tag{17}$$

In the very-weak and strong limit this reduces respectively to $w = 2u^2/\alpha_L \hbar^2$ and $w = |u|/\hbar$. Eqns. 16 and 17 are plotted in Fig. 3 as interaction energy against α/w.

So far we have not specified the form of the interaction energy. For a point dipole-dipole interaction, $u \propto R^{-3}$ and thus the transfer rate varies as R^{-3} for strong

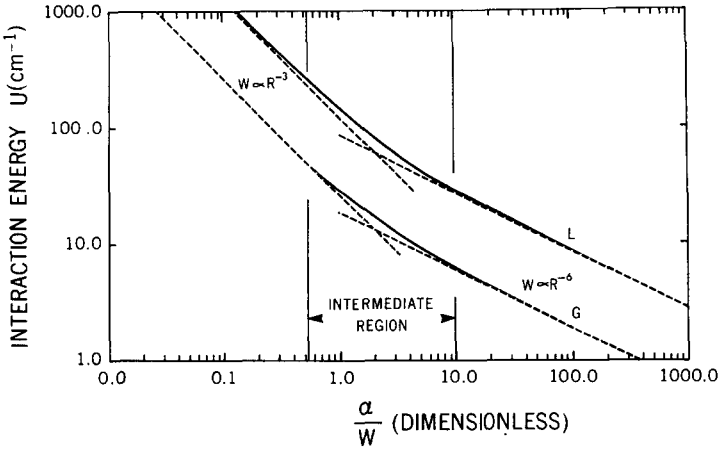

Fig. 3. Solution of the generalized master equation for Gaussian (G) and Lorentzian (L) absorption profiles (Eqns. 16 and 17). The dotted lines are the asymptotes corresponding to the limits of strong and very-weak coupling.

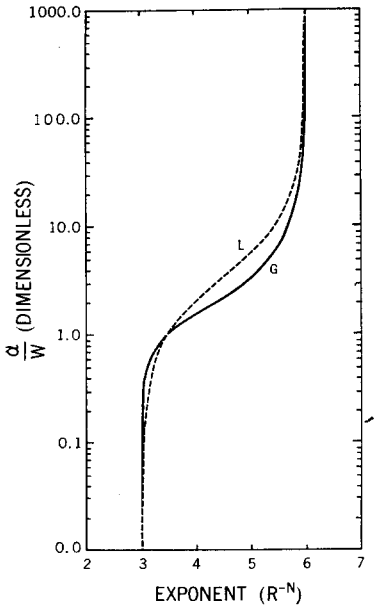

Fig. 4. The variation of transfer rate with molecular separation expressed as R^{-N} as a function of α/w as given by the generalized master equation Eqn. 18, assuming dipole-dipole interaction for Gaussian (G) and Lorentzian (L) absorption profiles.

coupling and R^{-6} for very-weak coupling for both Gaussian and Lorentzian profiles.

If we wish to assume in the intermediate region a transfer rate proportional to R^{-N}, it is readily shown [7] that

$$N = \begin{cases} 6\left[1+\dfrac{\exp(-\alpha_G^2/w^2)-1}{\sqrt{\pi}(\alpha_G/w)\,\mathrm{erf}\,(\alpha_G/w)}\right] & \text{Gaussian} \\ 6[\{1-\exp(-\alpha_L/w)\}^{-1}-w/\alpha_L] & \text{Lorentzian} \end{cases} \tag{18}$$

The exponent N as a function of α/w is plotted in Fig. 4.

V. APPLICATION TO PHOTOSYNTHESIS

We shall now determine the parameter α from the monomer absorption spectrum of chlorophyll *a* in ether. The halfwidth of the 660 nm band is 188 cm^{-1} [1], thus for a single Gaussian and Lorentzian component we obtain from Eqn. 10: $\alpha_G = 4.79\times10^{12}\ s^{-1}$ and $\alpha_L = 1.13\times10^{13}\ s^{-1}$. If we include the 613 nm satellite we must rework Eqn. 9 for two components. This we have done numerically [7] for the spectrum in Fig. 4 fitted with two Gaussians. $\phi(t)$ for the double Gaussian falls quickly into line with the value computed for a single Gaussian at 660 nm (Fig. 5). The satellite does very little to change $\phi(t)$ other than for a small oscillation at the beginning, which would not change the value of α significantly. Thus we will use the above values for α. Knowing α we can now determine transfer rates as a function of interaction energy. These have been plotted in Fig. 6 for a Gaussian and Lorentzian profile with the same halfwidth. The curves illustrate the extent to which the transfer

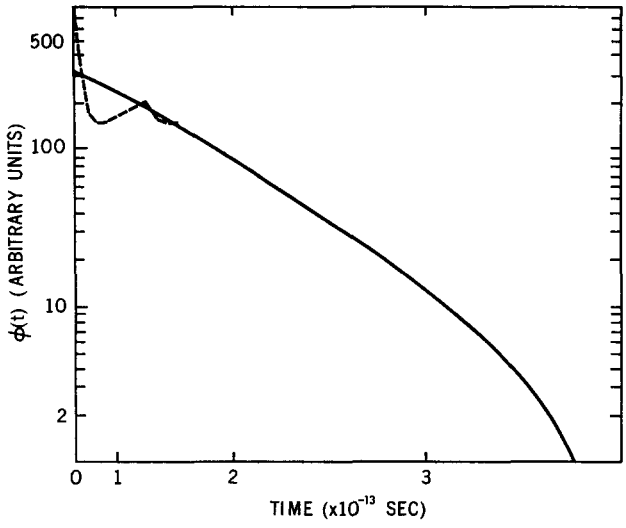

Fig. 5. Comparison of the memory function ϕ for a single Gaussian absorption band at 660 nm (solid line) and a double Gaussian absorption band at 660 nm and 613 nm (dotted line).

may be described by very-weak and strong coupling theory, and the connection between the two in the intermediate or weak coupling region. A characteristic of the Gaussian profile is the shorter extent of the very-weak coupling region and a faster approach to the strong coupling asymptote as compared to the Lorentzian profile.

The energy transfer process is Markoffian if the memory function is very small

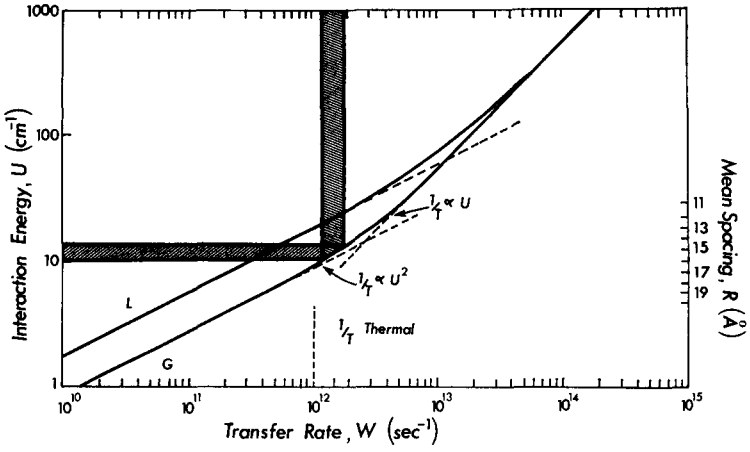

Fig. 6. Transfer rate versus interaction energy as predicted by the generalized master equation solution (Eqn. 16) for the 660 nm band of chlorophyll *a* fitted with a Gaussian profile, G. Curve L is a Lorentzian fit (Eqn. 17) for comparison. The shaded region indicates the range of transfer rates deduced from the experimental fluorescence lifetimes. The mean-spacing values correspond to the chlorophyll *a* separation needed to produce the interaction energies on the left-hand axis assuming a dipole-dipole approximation and the dipole orientation of 35° with the plane of the membrane. The asymptotes for the limits of strong and very-weak coupling are shown, and also the rate corresponding to thermal relaxation (dotted lines).

for times of order $1/w$. The excitation then hops from site to site and the trapping time is

$$\tau_t = \langle n \rangle \tau_j \tag{19}$$

where $\langle n \rangle$ is the average number of steps taken to reach the trap and the nearest neighbor transfer time τ_j is equal to $1/w$, the reciprocal of the transfer rate. Montroll [28] obtained the asymptotic expression for the average number of steps in a random walk on a two-dimensional lattice with one trap:

$$\langle n \rangle = N \ln N/\pi + 0.195056N + \ldots \tag{20}$$

where N is the number of lattice points, in this case antenna chlorophyll.

Eqns. 19 and 20 are only applicable if $\alpha/w > 10$ as shown in Fig. 3. However we expect that three factors would destroy the coherent nature of exciton transport and lead to a diffusion of energy rather than wave-like propagation: (1) Irregular chlorophyll spacing, (2) the fact that the chlorophyll orientation is likely to vary somewhat, and (3) chlorophyll molecules are polyatomic and therefore having a high density of vibrational states, lend themselves to large exciton-phonon scattering in the lipid medium.

The effect of random spacing and orientation on the scattering of excitons was investigated by Katsuura [29] for a one-dimensional lattice of dipoles with strong coupling. He calculated the time dependence of the root mean square displacement of excitation for varying degrees of variance in the lattice spacing and orientation of the dipoles and, he found that the root mean square displacement soon becomes dependent on the square root of time as required for diffusion.

In the weak coupling region the coherent propagation is even more sensitive to disruption [3]. We therefore assume the random walk equation to be applicable for our model.

Assuming 250 to 350 antenna chlorophyll in Photosystem II, the average number of transfers to reach the trap (Eqn. 20) is 488 to 721, which by Eqn. 19 gives a transfer rate of

$$w = 1.2 \times 10^{12}\ \mathrm{s}^{-1} \text{ to } 1.8 \times 10^{12}\ \mathrm{s}^{-1}$$

This range of w corresponds to a range of interaction energy predicted by the generalized master equation theory (Eqn. 16 or Fig. 6) of $u = 10$ to $13\ \mathrm{cm}^{-1}$. The lower value corresponds to 250 antenna chlorophyll and the upper value to 350.

We shall now calculate u independently from the model assumptions of mean spacing and orientation, and the chlorophyll *a* absorption spectrum as discussed in Section II. If the interaction is entirely dipole-dipole, it is given by [3]

$$u = M^2 K / n^2 R^3 \tag{21}$$

Here $n = 1.45$ is the refractive index. We shall calculate u for a range of R from 14 to 16 Å, the assumed mean spacing of chlorophyll *a* in Photosystem II. $K = \cos\theta - 3\cos\phi\cos\psi$, where θ is the angle between the dipoles and ϕ, ψ are the angles the dipoles make with the line joining them. If the transition moments are allowed to rotate azimuthally maintaining an angle β with the plane of the membrane, the mean square average of K is

$$\langle K^2 \rangle = \sin^4\beta + \tfrac{5}{4}\cos^4\beta. \tag{22}$$

For an orientation of the transition moment $\beta = 35 \pm 2°$ the root mean square value of K is 0.82 ± 0.02. The transition dipole moment M is obtained from the absorption spectrum [30]:

$$M^2 = 9.184 \times 10^{-39} \int \varepsilon(\nu) d\nu / \nu_a \tag{23}$$

where $\varepsilon(\nu)$ is the extinction coefficient ($cm^{-1} \cdot mol^{-1} \cdot l$) as a function of wavenumber ν (cm^{-1}), and ν_a is the absorption maximum.

For a Gaussian line shape this becomes

$$M^2 = 1.955 \times 10^{-38} \varepsilon_m \nu_{\frac{1}{2}} / \nu_a \tag{24}$$

where ε_m is the extinction coefficient at the maximum. For chlorophyll *a* in ether we have[1] $\varepsilon_m = 85\,100\ cm^{-1} \cdot mol^{-1} \cdot l$, $\nu_{\frac{1}{2}} = 188\ cm^{-1}$, and $\nu_a = 15\,149\ cm^{-1}$. Thus we obtain $M^2 = 2.07 \times 10^{-35}$ esu.

The interaction energy (Eqn. 21) has been plotted in Fig. 7 for a range of antenna spacings R.

We can also obtain some estimate of the error involved in using the dipole-dipole approximation. Chang [31] has worked out a correction to the dipole-dipole approximation. An exact calculation of the transition monopoles [31], which involves calculating orbital wavefunctions, shows that for $R = 15 \pm 1$ Å the ratio of exact interaction to dipole-dipole calculation for chlorophyll *a* varies from 0.7 to 1.4 depending on the orientation. This means that the interaction energy calculated from

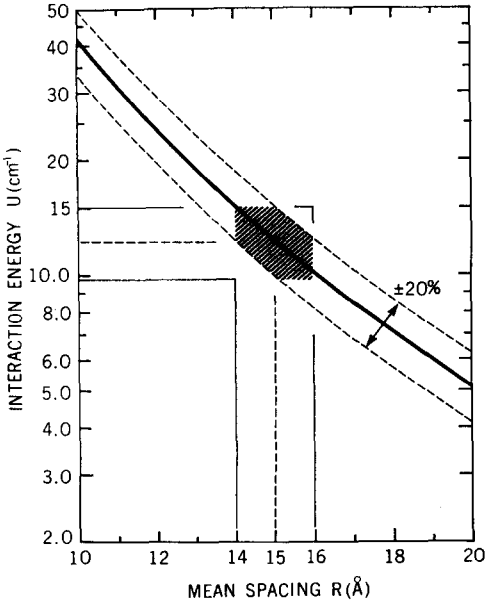

Fig. 7. Energy versus chlorophyll *a* separation for dipole-dipole interaction (Eqn. 21). The possible ± 20 % correction for the exact monopole calculation is indicated.

Eqn. 21 may differ by an additional $\pm 20\,\%$. Together with the range of R from 14 to 16 Å this leads to a range of interaction energy $u = 10$ to $15\ \mathrm{cm}^{-1}$, which is in good agreement with the 10 to 13 cm^{-1} predicted by the generalized master equation for our model.

Substituting the calculated interaction energy of 10 to 15 cm^{-1} into the generalized master equation solution (Eqn. 16) we obtain the nearest neighbor transfer rate

$$w = 1.1 \times 10^{12}\ \mathrm{s}^{-1} \text{ to } 2.1 \times 10^{12}\ \mathrm{s}^{-1}.$$

We can compare this to the pair-wise transfer rate predicted by the Förster theory for the same range of interaction energy, and the same mean-spacing and orientation assumptions as in our model. Using a Förster parameter of $R_0 = 65.1$ Å, based on spectroscopic measurements of chlorophyll-*a* in lipid vesicles [31], Colbow [1] obtained

$$w = 0.24 \times 10^{12}\ \mathrm{s}^{-1} \text{ to } 0.64 \times 10^{12}\ \mathrm{s}^{-1}$$

As expected, this is somewhat lower than the predictions of the generalized master equation as the rates from the Förster theory fall in the very-weak coupling region but near the intermediate region where the R^{-6} rate dependence applies (Fig. 6). Thus the generalized master equation theory gives better agreement with the transfer rates of $1.2 \times 10^{12}\ \mathrm{s}^{-1}$ to $1.8 \times 10^{12}\ \mathrm{s}^{-1}$ deduced from the fluorescent lifetime with the assumption of random walk among 250–350 antenna molecules per trap. The generalized master equation also provides an expression useful for calculating transfer rates over a wide range of interaction strengths.

ACKNOWLEDGEMENT

This work was supported by the National Research Council of Canada.

REFERENCES

1 Colbow, K. (1973) Biochim. Biophys. Acta 314, 320–327
2 Simpson, W. T. and Peterson, D. L. (1957) J. Chem. Phys. 26, 588–593
3 Förster, Th. (1967) Comprehensive Biochemistry 22, 61–80; (1965) in Modern Quantum Chemistry (Sinanogulu, 0. ed.) Vol. III, pp. 93–137, Academic Press, New York
4 Borisov, A. Yu. and Il'ina, M. D. (1973) Biochim. Biophys. Acta 305, 364–371
5 Siebart, M. and Alfano, R. R. (1974) Biophys. J. 14, 169–283
6 Kenkre, V. M. and Knox, R. S. (1974) Phys. Rev. B 9, 5279–5290; (1974) Phys. Rev. Lett. 33, 803–806
7 Danyluk R. P. (1975) M. Sc. Thesis, Simon Fraser University
8 Katz, J. J. (1973) Naturwissenschaften 60, 32–39
9 Pearlstein, R. M. (1967) Brookhaven Natl. Symp. 19, 8–15
10 French, C. S. (1960) in Handbuch der Pflanzenphysiologie (Ruhland, W., ed.), Vol. 5, pp. 252–297, Springer, Berlin
11 Clayton, R. K. (1965) Molecular Physics in Photosynthesis, Blaisdel, New York
12 Goedheer, J. C. (1966) in The Chlorophylls (Vernon and Seely, eds.), pp. 147–184, Academic Press, New York
13 Kreutz, W. (1970) Adv. Bot. Res. 3, 53–169
14 Steinemann, A., Stark, G. and Läuger, P. (1972) J. Membrane Biol. 9, 177–194
15 Cherry, R. J., Hsu, K. and Chapman, D. (1972) Biochim. Biophys. Acta 267, 512–522

16 Hoff, A. J. (1974) Photochem. Photobiol. 19, 51–57
17 Wolken, J. J. and Schwertz, F. A. (1953) J. Gen. Physiol. 37, 111–119
18 Thomas, J. B., Minnaert, K. and Elbers, P. F. (1955) Acta Bot. Neerl. 5, 315–321
19 Emerson, R. and Arnold, W. (1932) J. Gen. Physiol. 15, 391–420; ibid, 16, 191–205
20 Rabinowitch, E. and Govindjee (1969) in Photosynthesis, Wiley, New York
21 Schmid, G. H. and Gaffron, H. (1968) J. Gen. Physiol. 52, 212–239; (1969) Prog. Photosynthesis Res. 2, 857–870; (1971) Photochem. Photobiol. 14, 451–464
22 Hoch, G. and Knox, R. S. (1968) in Photophysiology (Giese, A. C., ed.), Vol. 3, pp. 225–251, Academic Press, New York
23 Müller, A., Lumry, R. and Walker, M. S. (1969) Photochem. Photobiol. 9, 113–126
24 Borisov, A. Yu. and Godik, V. I. (1973) Biochim. Biophys. Acta 301, 227–248
25 Goedheer, J. C. (1972) Ann. Rev. Plant Physiol. 23, 87–112
26 Clayton, R. K. (1972) Proc. Natl. Acad. Sci. U.S.A. 69, 44–49
27 Knox, R. S. (1968) J. Theor. Biol. 21, 244–252
28 Montroll, E. W. (1969) J. Math. Phys. 10, 753–765
29 Katsuura, K. (1964) J. Chem. Phys. 40, 3527–3530
30 McRae and Kasha, M. (1964) in Physical Processes in Radiation Biology, pp. 23, Academic Press, New York
31 Chang, J. C. (1972) Ph. D. Thesis, University of Rochester, New York
32 Colbow, K. (1973) Biochim. Biophys. Acta 318, 4–9
33 Breton, J., Michel-Villas, M. and Paillotin, G. (1973) Biochim. Biophys. Acta 314, 42–56
34 Paschenko, V. Z., Protasov, S. P., Rubin, A. B., Timofeev, K. N., Zamazova, L. M. and Rubin, L. B. (1975) Biochim. Biophys. Acta 408, 143–153
35 Beddard, G. S., Porter, G. and Tredwell, C. J. (1975) Nature 258, 166–168